

L-284
NATIONAL ADVISORY COMMITTEE FOR AERONAUTICS

WARTIME REPORT

ORIGINALLY ISSUED

May 1946 as
Advance Restricted Report L6C19

COLUMN AND PLATE COMPRESSIVE STRENGTHS

OF AIRCRAFT STRUCTURAL MATERIALS

EXTRUDED 14S-T ALUMINUM ALLOY

By George J. Heimerl and Donald E. Niles

Langley Memorial Aeronautical Laboratory
Langley Field, Va.



WASHINGTON

NACA WARTIME REPORTS are reprints of papers originally issued to provide rapid distribution of advance research results to an authorized group requiring them for the war effort. They were previously held under a security status but are now unclassified. Some of these reports were not technically edited. All have been reproduced without change in order to expedite general distribution.

NATIONAL ADVISORY COMMITTEE FOR AERONAUTICS

ADVANCE RESTRICTED REPORT

COLUMN AND PLATE COMPRESSIVE STRENGTHS
OF AIRCRAFT STRUCTURAL MATERIALS

EXTRUDED 14S-T ALUMINUM ALLOY

By George J. Heimerl and Donald E. Niles

SUMMARY

Column and plate compressive strengths of extruded 14S-T aluminum alloy were determined both within and beyond the elastic range from tests of flat-end H-section columns and from local-instability tests of H-, Z-, and channel-section columns. These tests are part of an extensive research investigation to provide data on the structural strength of various aircraft materials. The results are presented in the form of curves and charts that are suitable for use in the design and analysis of aircraft structures.

INTRODUCTION

Column and plate members that fail by instability are basic elements in an aircraft structure. For the design of structurally efficient aircraft, the strength of these elements must be known for the various aircraft materials. An extensive research program has therefore been undertaken at the Langley Memorial Aeronautical Laboratory to establish the column and plate compressive strengths of a number of the alloys available for use in aircraft structures. Parts of this investigation have been completed; the alloys already investigated include 24S-T and 17S-T aluminum-alloy sheet and extruded 75S-T, 24S-T, and F303-T aluminum alloys (references 1 to 5, respectively).

Because of the increased interest in the use of extruded 14S-T aluminum alloy, this alloy has been included in the investigation. The results of tests to determine the column and plate compressive strengths of extruded 14S-T aluminum alloy are presented herein.

SYMBOLS

L	length of column
ρ	radius of gyration
c	fixity coefficient used in Euler column formula
$\frac{L}{\rho\sqrt{c}}$	effective slenderness ratio of column
b_F, t_F	width and thickness, respectively, of flange of H-, Z-, or channel section (see fig. 1)
b_W, t_W	width and thickness, respectively, of web of H-, Z-, or channel section (see fig. 1)
r	radius of corner fillet (see fig. 1)
k_W	nondimensional coefficient used with b_W and t_W in plate-buckling formula (see figs. 2 and 3 taken from reference 6)
E_c	modulus of elasticity in compression, taken as 10,700 ksi for extruded 14S-T aluminum alloy
τ	nondimensional coefficient (The value of τ is so determined that, when the effective modulus of elasticity τE_c is substituted for E_c in the equation for elastic buckling of columns, the computed critical stress agrees with the experimentally observed value. The coefficient τ is equal to unity within the elastic range and decreases with increasing stress beyond the elastic range.)
η	nondimensional coefficient for compressed plates corresponding to τ for columns

μ Poisson's ratio, taken as 0.3 for extruded 14S-T aluminum alloy

σ_{cr} critical compressive stress

$\bar{\sigma}_{max}$ average compressive stress at maximum load

σ_{cy} compressive yield stress

METHOD OF TESTING AND ANALYSIS

All tests were made in hydraulic testing machines accurate within three-fourths of 1 percent.

Stress-strain curves. - The compressive stress-strain curves, which identify the material for correlation with its column and plate compressive strengths, were obtained for the with-grain direction for both ends of the 20-foot extrusions used to make the columns. For the flat-end columns used to determine the column strength, compression stress-strain specimens, 2.5 inches long and of the identical cross section as the columns, were used to obtain an average stress-strain curve applicable to the entire column cross section; no lateral supports were required for these specimens because buckling did not occur before the yield stress was reached. For the columns used to determine the plate compressive strength, an average stress-strain curve for the entire column cross section could not be obtained from similar full-size cross-sectional specimens because buckling would have occurred before the stress reached the yield value. For this reason, single-thickness compression specimens were cut from the middle of the web, and from the parts of the flanges immediately adjacent to the corner fillets at the junction of the flange and web. The single-thickness specimens were tested in a Montgomery-Templin type of compression fixture, which provides lateral support to the specimen through closely spaced rollers. (See reference 7 for the technique in using this type of fixture.) Tuckerman strain gages (1-in. gage length) were used to measure strains for both types of compression specimens.

Column strength. - The column strength and the associated effective column modulus of elasticity were obtained from tests of flat-end H-section columns with the fixity coefficient c assumed to be equal to 4. The columns were tested with the ends ground flat and square and bearing directly against the testing-machine heads. The nominal cross-sectional dimensions for all the columns were $b_F = 0.56$, $b_W = 1.64$, and $t_F = t_W = 0.125$ inch. This size of section was obtained by milling off the necessary amount from the flanges of an extruded H-section and was chosen so that the columns would develop a higher local-instability strength than the greatest column strength expected.

The crookedness of the columns, the distance from a point at the midpoint of the column from a straight line drawn between corresponding points at the ends of the column, was measured by means of a plane surface and a moveable dial-gage setup. The ratio of length to crookedness was greater than 1000 in all cases. (The strength of columns with this ratio less than 1000 may be noticeably reduced by the crookedness of the column.) As some of the columns developed a tendency to twist after the flanges were machined down, this twist was removed before the crookedness was determined and before the column test was made. In order to measure the crookedness, the twist was removed by holding the flanges at each end of the column to bear firmly against uniformly thick steel blocks resting on the plane surface. Before the tests were made, the column was clamped against a guide bar at each end until a small initial load was applied, then the guide bars were removed.

Plate compressive strength. - The method of testing and analysis developed for this research program to determine the plate compressive strength (see reference 1) is briefly summarized as follows:

The plate compressive strength was obtained from compression tests of H-, Z-, and channel-section columns so proportioned as to develop local instability, that is, instability of the plate elements. (See fig. 4.) Extruded H-sections of three different web widths were tested; the flange widths for each were varied by milling off parts of the flanges. The flanges of some of the H-section extrusions were removed in such a way as to make Z- or channel sections as desired; the flange widths

of the Z- and channel-section columns were varied in the same manner as the flange widths for the H-section columns. The lengths of the columns were selected so as to obtain whenever possible a desirable three half-wave buckling pattern in accordance with the principles in reference 8. The tests were made with the column ends ground flat and square and bearing directly against the testing-machine heads. In these local-instability tests, measurements were taken of the cross-sectional distortion, and the critical stress was determined as the stress at the point near the top of the knee of the stress-distortion curve where a marked increase in distortion first occurred with small increase in stress.

The method of analysis presented herein differs from the method presented in reference 1 in that the inside face dimensions were used to define b_F and b_W . This definition of b_F and b_W for extruded sections with small fillets was previously used in references 3 to 5 in order that the theoretical and experimental buckling stresses would agree within the elastic range. For formed Z- and channel sections with an inside bend radius of three times the sheet thickness (references 1 and 2), b_F and b_W were defined as center-line widths with square corners assumed.

RESULTS AND DISCUSSION

Compressive Properties

The compressive stress-strain curves that apply to the extruded 11S-T aluminum alloy used in this investigation are summarized in figure 5. The variation in compressive yield stress shown by the dashed curves indicates the maximum differences that were found to exist between the average values obtained at the ends of the different 20-foot extrusions; in some cases, this variation was so small that only a single curve is shown. Curves A apply to the material used for the flat-end column tests, whereas curves B to E apply to that used for the local-instability tests. The columns to which the stress-strain curves B to E apply are identified by the letters given in tables 1, 2, and 3. The average value of σ_{cy} that applies to all the flat-end H-section columns is 57.0 ksi and to all the local-instability tests is 59.8 ksi for the flange material and 58.3 ksi for the web material.

The average values of σ_{cy} for the web were lower than those for the flange. In a few cases, however, individual values of σ_{cy} for the web were slightly higher than those obtained for the flange. A survey of σ_{cy} over a cross section of the largest extrusion (see fig. 6) showed that the values of σ_{cy} were lower in the outer than in the inner part of the flanges. Limited data on the intermediate-size extrusion indicated more uniform distribution of σ_{cy} over the flange widths than shown in figure 6. The variation of compressive yield strength shown, therefore, should not be regarded necessarily as typical for extrusions of this alloy.

Column and Plate Compressive Strengths

Because the compressive properties of an extruded aluminum alloy may vary considerably, the data and charts of this report should not be used for design purposes for extrusions of 14S-T aluminum alloy that have appreciably different compressive properties from those reported herein, unless a suitable method is devised for adjusting test results to account for variations in material properties. (Average values of σ_{cy} are given in round numbers on figs. 7 to 12.) The results of the column and local-instability tests of extruded 14S-T aluminum alloy are summarized herein; a discussion of basic relationships is given in reference 1.

Column strength. - The column curve of figure 7 shows the results of the flat-end H-section column tests. The reduction of the effective modulus of elasticity for columns τE_c with increase in stress is indicated by the variation of τ with stress shown in figure 8.

Plate-compressive strength. - The results of the local-instability tests of the H-, Z-, and channel-section columns used to determine the plate compressive strength are given in tables 1, 2, and 3, respectively.

The plate-buckling curve, analogous to the column curve of figure 7, is shown in figure 9. The reduction of the effective modulus of elasticity for plates ηE_c with increase in stress is indicated by the variation of η with stress, which is shown with the curve

for τ in figure 8. The τ - and η -curves diverge from unity at about the same value of stress; this deviation indicates that the H-, Z- and channel-section columns had about the same degree of imperfection as the flat-end H-section columns used to determine the column strength. This imperfection is apparent for both classes of columns because the η - and τ -curves diverge from unity at a stress below that for any visible divergence of the stress-strain curves from straight lines. (See fig. 5.)

The variation of the actual critical stress σ_{cr} with the theoretical critical stress σ_{cr}/η computed for elastic buckling by means of the formula and curves of figures 2 and 3 is shown in figure 10.

In order to illustrate the difference between the critical stress σ_{cr} and the average stress at maximum load $\bar{\sigma}_{max}$, the variation of σ_{cr} with $\sigma_{cr}/\bar{\sigma}_{max}$ is shown in figure 11. Because values of $\bar{\sigma}_{max}$ may be required in strength calculations, the variation of $\bar{\sigma}_{max}$ with σ_{cr}/η is shown in figure 12.

Attention is directed to the fact that a single plate curve appears on each of figures 9 to 12 whereas separate curves were found for H-sections and for Z- and channel sections in the corresponding figures for extruded 75S-T, 24S-T, and R303-T aluminum alloys in references 3, 4, and 5, respectively. The much greater scatter of the test data in figures 9 to 12, as compared with the corresponding figures given in references 3 to 5, makes it appear that one of the reasons for the failure to detect separate curves for this extruded 14S-T aluminum alloy may possibly be due to a variable distribution of the compressive yield stress over the cross section of the different extrusions, and hence may not have been the same as that shown in figure 6 for each extrusion. If the scatter had been less, and only a single plate curve obtained for this extruded 14S-T aluminum alloy, it would be reasonable to conclude that the type of distribution of the compressive yield stress over the cross section

was different from that found for the other extruded aluminum alloys (references 3 to 5).

Langley Memorial Aeronautical Laboratory
National Advisory Committee for Aeronautics
Langley Field, Va.

REFERENCES

1. Lundquist, Eugene E., Schuette, Evan H., Heimerl, George J., and Roy, J. Albert: Column and Plate Compressive Strengths of Aircraft Structural Materials. 24S-T Aluminum-Alloy Sheet. NACA ARR No. L5F01, 1945.
2. Heimerl, George J., and Roy, J. Albert: Column and Plate Compressive Strengths of Aircraft Structural Materials. 17S-T Aluminum-Alloy Sheet. NACA ARR No. L5F08, 1945.
3. Heimerl, George J., and Roy, J. Albert: Column and Plate Compressive Strengths of Aircraft Structural Materials. Extruded 75S-T Aluminum Alloy. NACA ARR No. L5F08a, 1945.
4. Heimerl, George J., and Roy, J. Albert: Column and Plate Compressive Strengths of Aircraft Structural Materials. Extruded 24S-T Aluminum Alloy. NACA ARR No. L5F08b, 1945.
5. Heimerl, George J., and Fay, Douglas P.: Column and Plate Compressive Strengths of Aircraft Structural Materials. Extruded R303-T Aluminum Alloy. NACA ARR No. L5H04, 1945.
6. Kroll, W. D., Fisher, Gordon P., and Heimerl, George J.: Charts for Calculation of the Critical Stress for Local Instability of Columns with I-, Z-, Channel, and Rectangular-Tube Section. NACA ARR No. 3K04, 1943.
7. Kotanchik, Joseph N., Woods, Walter, and Weinberger, Robert A.: Investigation of Methods of Supporting Single-Thickness Specimens in a Fixture for Determination of Compressive Stress-Strain Curves. NACA RE No. L5E15, 1945.
8. Heimerl, George J., and Roy, J. Albert: Determination of Desirable Lengths of Z- and Channel-Section Columns for Local-Instability Tests. NACA RB No. 14H10, 1944.

TABLE 1.- DIMENSIONS AND TEST RESULTS FOR EXTRUDED H-SECTION
COLUMNS THAT DEVELOP LOCAL INSTABILITY

Column	Applicable stress-strain curve (fig. 5)	t_w (in.)	t_F (in.)	b_w (in.)	b_F (in.)	L (in.)	$\frac{L}{b_w}$	$\frac{t_w}{t_F}$	$\frac{b_w}{t_w}$	$\frac{b_F}{b_w}$	κ_w (fig. 2)	$\frac{b_w}{t_w} \sqrt{\frac{12(1-\mu^2)}{k_w}}$	$\frac{\sigma_{cr}}{\eta}$ (ksi) (a)	σ_{cr} (ksi)	$\bar{\sigma}_{max}$ (ksi)	$\frac{\sigma_{cr}}{\bar{\sigma}_{max}}$
1a	B	0.125	0.129	1.61	0.81	6.44	4.0	0.96	12.91	0.505	2.73	25.8	158.4	59.7	65.2	0.916
1b		.125	.127	1.61	.81	6.52	4.1	.99	12.86	.505	2.63	26.2	153.8	60.5	65.0	.931
1c		.126	.127	1.60	.81	6.50	4.1	.99	12.70	.506	2.62	25.9	157.1	63.4	66.0	.961
2a		.124	.129	1.62	.90	7.58	4.7	.96	13.00	.556	2.36	28.0	135.1	58.5	63.5	.921
2b		.124	.129	1.62	.90	7.60	4.7	.96	13.02	.556	2.36	28.0	134.7	57.6	62.3	.925
2c		.124	.129	1.62	.90	7.50	4.6	.96	13.04	.555	2.37	28.0	134.8	58.5	61.8	.947
3a		.124	.129	1.62	.98	8.72	5.4	.96	13.07	.602	2.05	30.2	116.1	59.2	61.1	.969
3b		.124	.130	1.62	.98	8.70	5.4	.96	13.02	.603	2.04	30.1	116.4	58.4	61.6	.948
3c		.124	.128	1.62	.98	8.92	5.5	.97	13.10	.601	2.00	30.6	112.7	58.9	62.6	.941
4a		.124	.129	1.61	1.06	9.09	5.6	.96	12.97	.660	1.76	32.3	101.2	57.9	60.3	.960
4b		.124	.129	1.62	1.06	9.10	5.6	.96	13.03	.652	1.78	32.3	101.4	58.5	60.0	.975
4c		.124	.130	1.62	1.06	9.08	5.6	.96	13.05	.655	1.77	32.4	100.5	58.3	59.9	.973
5a		.124	.130	1.62	1.14	9.38	5.8	.96	13.03	.702	1.56	34.5	88.9	56.0	59.5	.941
5b		.124	.129	1.62	1.14	9.44	5.8	.96	13.03	.701	1.57	34.4	89.4	56.9	59.1	.963
6a		.125	.130	1.62	1.21	9.62	5.9	.96	13.01	.749	1.39	36.5	79.4	56.1	58.6	.957
6b		.125	.130	1.63	1.21	9.68	6.0	.96	13.06	.747	1.40	36.5	79.4	56.3	57.9	.972
6c		.124	.129	1.63	1.21	9.66	5.9	.96	13.08	.747	1.40	36.5	79.1	56.1	58.0	.967
7a		.124	.130	1.61	1.34	10.14	6.3	.96	12.95	.830	1.18	39.5	68.0	52.4	54.7	.958
7b		.125	.130	1.62	1.34	10.10	6.3	.96	12.96	.831	1.17	39.6	67.4	52.3	54.9	.953
7c		.124	.130	1.62	1.34	10.16	6.3	.96	13.03	.825	1.19	39.5	67.8	52.4	55.0	.953
8a	B	.121	.125	2.23	.90	8.92	4.0	.96	18.51	.404	3.80	31.4	107.3	57.9	60.6	.955
8b		.120	.125	2.24	.90	8.94	4.0	.96	18.63	.401	3.77	31.7	105.0	57.6	60.2	.957
8c		.120	.124	2.24	.90	8.90	4.0	.97	18.62	.403	3.75	31.8	104.6	58.2	60.5	.962
9a		.120	.125	2.24	1.01	10.08	4.5	.96	18.64	.452	3.24	34.2	90.2	58.0	59.7	.972
9b		.120	.125	2.24	1.01	10.08	4.5	.96	18.59	.452	3.24	34.1	90.7	58.1	59.7	.973
9c		.121	.124	2.23	1.01	10.06	4.5	.98	18.47	.453	3.14	34.4	89.0	56.5	59.9	.943
10a		.120	.125	2.24	1.13	11.23	5.0	.96	18.62	.504	2.77	37.0	77.3	55.6	56.8	.979
10b		.120	.125	2.24	1.13	11.26	5.0	.96	18.63	.504	2.76	37.1	76.9	55.6	57.1	.974
10c		.120	.125	2.24	1.13	11.26	5.0	.96	18.64	.504	2.76	37.1	76.8	55.0	57.4	.958
11a		.120	.124	2.25	1.35	12.12	5.4	.97	18.71	.598	2.04	43.3	56.4	50.9	52.2	.975
11b		.120	.124	2.24	1.35	12.14	5.4	.97	18.64	.602	2.03	43.2	56.5	51.4	52.4	.981
11c		.120	.124	2.24	1.35	12.17	5.4	.97	18.62	.603	2.01	43.4	56.1	51.0	52.7	.968
12a		.121	.125	2.23	1.58	12.94	5.8	.96	18.51	.707	1.54	49.3	43.5	41.5	45.7	.908
12b		.120	.125	2.24	1.58	12.96	5.8	.97	18.57	.705	1.54	49.4	43.2	42.8	45.7	.937
12c		.121	.125	2.23	1.58	12.94	5.8	.97	18.44	.706	1.54	49.1	43.8	41.9	45.6	.919
13a		.121	.125	2.23	1.83	14.08	6.3	.96	18.50	.823	1.20	55.8	33.9	32.6	42.7	.763
13b		.121	.125	2.23	1.83	14.20	6.4	.97	18.48	.822	1.20	55.8	34.0	33.6	42.7	.787

$$^a \frac{\sigma_{cr}}{\eta} = \frac{k_w n^2 E_c t_w^2}{12(1-\mu^2) b_w^2}, \text{ where } E_c = 10,700 \text{ ksi and } \mu = 0.3.$$

TABLE 1.- DIMENSIONS AND TEST RESULTS FOR EXTRUDED H-SECTION
COLUMNS THAT DEVELOP LOCAL INSTABILITY - Concluded

Column	Applicable stress-strain curve (fig. 5)	t_w (in.)	t_F (in.)	b_w (in.)	b_F (in.)	L (in.)	$\frac{L}{b_w}$	$\frac{t_w}{t_F}$	$\frac{b_w}{t_w}$	$\frac{b_F}{b_w}$	(fig. 2)	$\frac{b_w}{t_w} \sqrt{\frac{12(1-\mu^2)}{k_w}}$	$\frac{\sigma_{cr}}{\eta}$ (ksi) (a)	σ_{cr} (ksi)	$\bar{\sigma}_{max}$ (ksi)	$\frac{\sigma_{cr}}{\bar{\sigma}_{max}}$
14a	c	0.118	0.121	2.73	1.10	12.56	4.6	0.98	23.15	0.405	3.67	39.9	66.2	53.6	56.2	0.954
14b		.118	.120	2.73	1.10	12.54	4.6	.98	23.21	.401	3.68	40.0	66.1	54.1	56.3	.961
14c		.117	.120	2.74	1.10	12.54	4.6	.98	23.36	.401	3.68	40.3	65.2	54.4	56.4	.965
15a		.119	.120	2.73	1.24	13.16	4.8	.99	22.95	.455	3.07	43.3	56.4	50.1	52.3	.958
15b		.119	.121	2.72	1.24	13.08	4.8	.98	22.96	.456	3.08	43.2	56.5	50.7	52.5	.966
15c		.119	.121	2.73	1.24	13.22	4.9	.98	22.94	.455	3.07	43.3	56.4	51.0	52.9	.964
16a		.118	.120	2.74	1.37	13.64	5.0	.98	23.30	.498	2.72	46.7	48.5	44.4	48.5	.915
16b		.118	.120	2.74	1.37	13.59	5.0	.98	23.32	.501	2.71	46.8	48.2	46.4	48.7	.953
16c		.118	.120	2.74	1.37	13.86	5.1	.98	23.26	.500	2.71	46.7	48.4	46.5	49.5	.939
17a		.119	.121	2.74	1.66	14.70	5.4	.98	23.07	.604	1.98	54.2	36.0	34.5		
17b		.118	.121	2.74	1.65	14.76	5.4	.98	23.25	.604	1.98	54.6	35.4	34.9	44.1	.791
18a		.119	.121	2.74	1.92	15.99	5.8	.98	23.05	.700	1.53	61.6	27.8	26.1	42.5	.614
18b		.118	.121	2.73	1.92	15.93	5.8	.98	23.19	.703	1.52	62.2	27.3	27.6	42.1	.656
18c		.120	.121	2.74	1.92	16.42	6.0	1.00	22.78	.701	1.49	61.6	27.8	25.9	41.9	.618
19a		.118	.121	2.74	2.24	17.28	6.3	.97	23.20	.818	1.17	70.9	21.0	20.5	39.2	.523
19b		.118	.122	2.75	2.24	17.26	6.3	.96	23.28	.817	1.18	70.8	21.1	19.5	39.2	.497
19c		.118	.123	2.74	2.24	17.23	6.3	.96	23.29	.818	1.18	70.8	21.0	20.5	39.6	.518

$$\frac{a\sigma_{cr}}{\eta} = \frac{k_w \pi^2 E_c t_w^2}{12(1-\mu^2) b_w^2}, \text{ where } E_c = 10,700 \text{ ksi and } \mu = 0.3.$$

NATIONAL ADVISORY
COMMITTEE FOR AERONAUTICS

TABLE 2.- DIMENSIONS AND TEST RESULTS FOR EXTRUDED Z-SECTION

COLUMNS THAT DEVELOP LOCAL INSTABILITY

Column	Applicable stress-strain curves (fig. 5)	t_w (in.)	t_F (in.)	b_w (in.)	b_F (in.)	L (in.)	$\frac{L}{b_w}$	$\frac{t_w}{t_F}$	$\frac{b_w}{t_w}$	$\frac{b_F}{b_w}$	k_w (fig. 3)	$\frac{b_w}{t_w} \sqrt{\frac{12(1-\mu^2)}{k_w}}$	$\frac{\sigma_{cr}}{\eta}$ (ksi) (a)	σ_{cr} (ksi)	$\bar{\sigma}_{max}$ (ksi)	$\frac{\sigma_{cr}}{\bar{\sigma}_{max}}$
1a	B	0.126	0.128	1.61	0.98	6.49	4.0	0.98	12.85	0.610	2.19	28.7	128.3	60.3	62.9	0.959
1b		.127	.129	1.61	.99	6.45	4.0	.98	12.73	.615	2.16	28.6	128.9	61.0	63.1	.967
1c		.121	.129	1.61	.98	6.50	4.0	.94	13.35	.607	2.35	28.8	127.5	59.2	61.6	.961
2a		.126	.128	1.61	1.07	7.31	4.5	.98	12.85	.662	1.93	30.6	113.1	58.9	62.2	.947
2b		.122	.131	1.61	1.06	7.30	4.5	.94	13.17	.659	2.04	30.5	113.8	57.7	60.7	.951
2c		.125	.128	1.62	1.06	7.25	4.5	.98	12.91	.653	1.96	30.5	113.7	58.8	60.9	.966
3		.126	.128	1.61	1.16	8.08	5.0	.98	12.86	.716	1.69	32.7	98.8	57.5	60.3	.954
4a		.124	.127	1.62	1.34	8.05	5.0	.98	13.01	.827	1.32	37.4	75.4	54.7	57.0	.960
4b		.125	.127	1.62	1.34	8.04	5.0	.98	12.96	.826	1.32	37.3	76.0	53.5	56.6	.945
5a		.124	.127	1.62	1.34	9.76	6.0	.98	13.02	.827	1.32	37.4	75.3	56.1	57.8	.971
5b	↓	.124	.127	1.62	1.34	9.75	6.0	.98	13.00	.829	1.31	37.5	75.0	54.5	57.1	.954
6a	B	.120	.126	2.22	1.14	10.10	4.6	.95	18.48	.514	2.99	35.3	84.7	54.5	57.0	.956
6b		.120	.124	2.22	1.14	10.19	4.5	.97	18.52	.512	2.93	35.0	82.6	55.3	57.0	.970
7a		.119	.123	2.23	1.37	12.20	5.5	.97	18.70	.616	2.18	41.9	60.3	52.1	53.1	.981
7b		.119	.125	2.22	1.37	12.18	5.5	.95	18.64	.617	2.25	41.1	62.6	52.8	53.8	.981
8a		.119	.123	2.23	1.60	13.00	5.9	.97	18.76	.717	1.70	47.5	46.7	44.2	47.1	.938
8b		.119	.125	2.22	1.63	12.99	5.9	.95	18.69	.735	1.67	47.8	46.2	44.2	47.1	.938
8c		.119	.125	2.22	1.63	13.00	5.9	.95	18.70	.732	1.68	47.7	46.5	46.4	48.0	.967
9a		.119	.125	2.22	1.86	14.20	6.4	.95	18.71	.838	1.33	53.6	36.7	36.7	42.5	.864
9b	↓	.119	.125	2.22	1.86	14.21	6.4	.95	18.69	.840	1.32	53.8	36.5	36.5	42.7	.855
10a	E	.120	.120	2.74	1.14	12.44	4.5	1.00	22.85	.415	3.62	39.7	67.1	53.8	56.3	.956
10b		.120	.123	2.73	1.14	12.49	4.6	.98	22.80	.417	3.68	39.2	68.5	54.8	58.1	.943
11a		.120	.123	2.74	1.40	13.68	5.0	.98	22.83	.511	2.89	44.4	53.6	49.5	51.0	.971
11b		.120	.122	2.74	1.39	13.65	5.0	.98	22.89	.507	2.91	44.3	53.7	48.2	50.1	.962
11c		.120	.120	2.74	1.38	13.68	5.0	1.00	22.86	.504	2.89	44.4	53.5	47.9	49.7	.964
12a		.120	.121	2.74	1.65	14.82	5.4	.99	22.88	.604	2.19	51.1	40.5	39.5	44.3	.892
12b		.120	.121	2.74	1.66	14.76	5.4	.99	22.84	.607	2.16	51.4	40.0	37.7	44.1	.855
12c		.120	.120	2.74	1.66	14.80	5.4	1.00	22.77	.606	2.16	51.3	40.3	38.8	43.5	.892
13a	E	.120	.121	2.74	2.25	17.17	6.3	.99	22.78	.822	1.31	65.8	24.4	23.2	39.4	.589

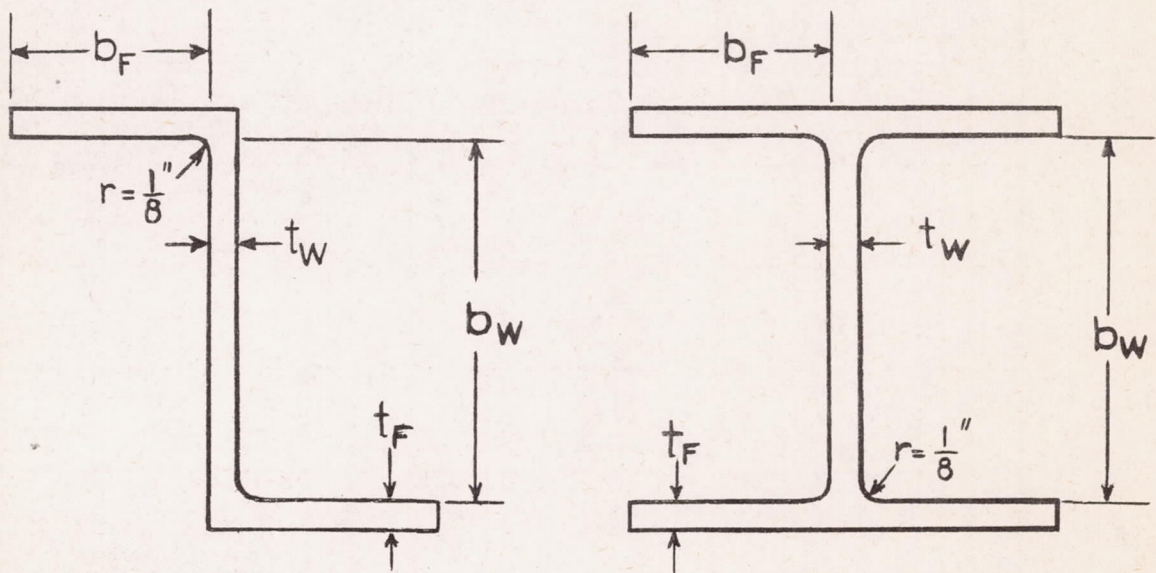
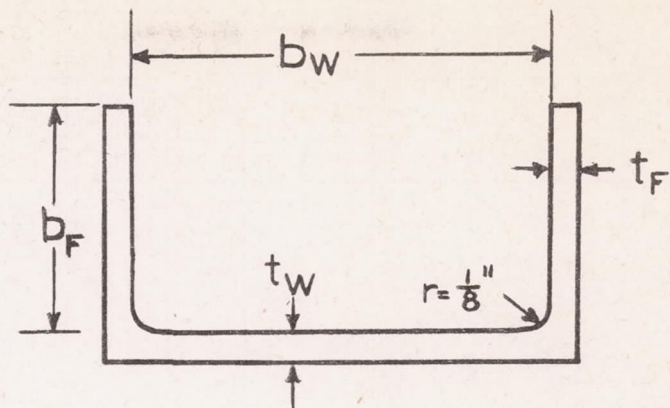
$$^a \frac{\sigma_{cr}}{\eta} = \frac{k_w \pi^2 E_c t_w^2}{12(1-\mu^2) b_w^2}, \text{ where } E_c = 10,700 \text{ ksi and } \mu = 0.3.$$

TABLE 3.- DIMENSIONS AND TEST RESULTS FOR EXTRUDED CHANNEL-SECTION
COLUMNS THAT DEVELOP LOCAL INSTABILITY

Column	Applicable stress-strain curve (fig. 5)	t_w (in.)	t_F (in.)	b_w (in.)	b_F (in.)	L (in.)	$\frac{L}{b_w}$	$\frac{t_w}{t_F}$	$\frac{b_w}{t_w}$	$\frac{b_F}{b_w}$	k_w (fig. 3)	$\frac{b_w}{t_w} \sqrt{\frac{12(1-\mu^2)}{k_w}}$	$\frac{\sigma_{cr}}{\eta}$ (ksi) (a)	σ_{cr} (ksi)	$\bar{\sigma}_{max}$ (ksi)	$\frac{\sigma_{cr}}{\bar{\sigma}_{max}}$
1a	B	0.121	0.129	1.61	0.98	6.48	4.0	0.94	13.34	0.606	2.36	28.7	128.2	57.8	61.0	0.948
1b		.120	.129	1.61	.97	6.49	4.0	.93	13.39	.601	2.40	28.6	129.5	57.8	60.8	.951
2a		.126	.128	1.61	1.07	7.26	4.5	.98	12.82	.666	1.92	30.5	112.9	58.4	60.2	.970
2b		.126	.128	1.61	1.07	7.30	4.5	.98	12.83	.662	1.91	30.7	112.2	57.7	61.5	.938
3a		.126	.128	1.62	1.14	8.08	5.0	.98	12.87	.708	1.73	32.4	101.0	56.6	60.1	.942
3b		.125	.128	1.62	1.14	8.07	5.0	.98	12.91	.706	1.73	32.4	100.4	55.7	60.2	.925
4a		.126	.128	1.61	1.34	9.79	6.1	.98	12.81	.833	1.29	37.3	76.0	53.1	56.8	.935
4b		.125	.128	1.61	1.33	9.87	6.1	.98	12.87	.824	1.33	36.9	77.7	54.2	57.0	.951
4c		.126	.128	1.61	1.34	9.81	6.1	.98	12.86	.827	1.30	37.3	76.0	52.6	57.1	.921
4d		.124	.128	1.61	1.34	9.80	6.1	.97	12.98	.830	1.31	37.5	75.2	52.7	56.8	.928
5a	B	.121	.124	2.22	1.14	10.12	4.6	.97	18.37	.512	2.91	35.6	83.4	55.1	56.9	.968
5b		.121	.124	2.22	1.14	10.10	4.5	.97	18.38	.513	2.91	35.6	83.3	54.2	56.6	.958
5c		.121	.124	2.22	1.13	10.12	4.6	.98	18.36	.509	2.91	35.6	83.5	54.2	56.7	.956
6a		.121	.124	2.22	1.36	12.21	5.5	.98	18.32	.613	2.19	40.9	63.1	51.1	52.7	.970
6b		.121	.124	2.22	1.36	12.21	5.5	.98	18.32	.612	2.19	41.0	62.9	49.5	51.5	.961
6c		.121	.124	2.22	1.36	12.17	5.5	.97	18.37	.612	2.19	41.0	62.8	49.4	51.7	.956
7a		.121	.124	2.22	1.59	12.98	5.8	.98	18.33	.717	1.69	46.6	48.6	43.9	45.6	.963
7b		.121	.124	2.22	1.60	12.99	5.8	.98	18.35	.720	1.67	46.9	48.0	44.5	45.7	.974
7c		.121	.124	2.22	1.60	13.00	5.9	.98	18.33	.720	1.67	46.9	48.1	43.5	45.2	.962
8a		.121	.125	2.22	1.84	14.18	6.4	.97	18.33	.828	1.31	52.9	37.7	37.2	43.5	.855
8b		.121	.124	2.22	1.84	14.18	6.4	.98	18.31	.828	1.31	52.9	37.8	36.5	43.2	.845
8c		.122	.124	2.22	1.84	14.16	6.4	.98	18.28	.828	1.31	52.8	37.9	36.9	43.3	.852
9a	D	.120	.122	2.74	1.12	12.50	4.6	.98	22.76	.408	3.71	39.1	69.3	51.6	55.5	.937
9b		.120	.123	2.73	1.11	12.51	4.6	.98	22.71	.407	3.72	38.9	69.8	52.3	55.8	.938
9c		.121	.122	2.74	1.11	12.50	4.6	.99	22.71	.406	3.72	38.9	69.8	52.3	55.3	.946
10		.120	.121	2.74	1.37	13.67	5.0	.99	22.89	.501	2.93	44.2	54.1	46.2	48.1	.960
11a	E	.120	.121	2.74	2.24	17.26	6.3	.99	22.78	.818	1.32	65.5	24.6	23.0	39.8	.578
11b		.121	.121	2.74	2.24	17.27	6.3	.99	22.72	.818	1.32	65.3	24.7	22.0	40.4	.545

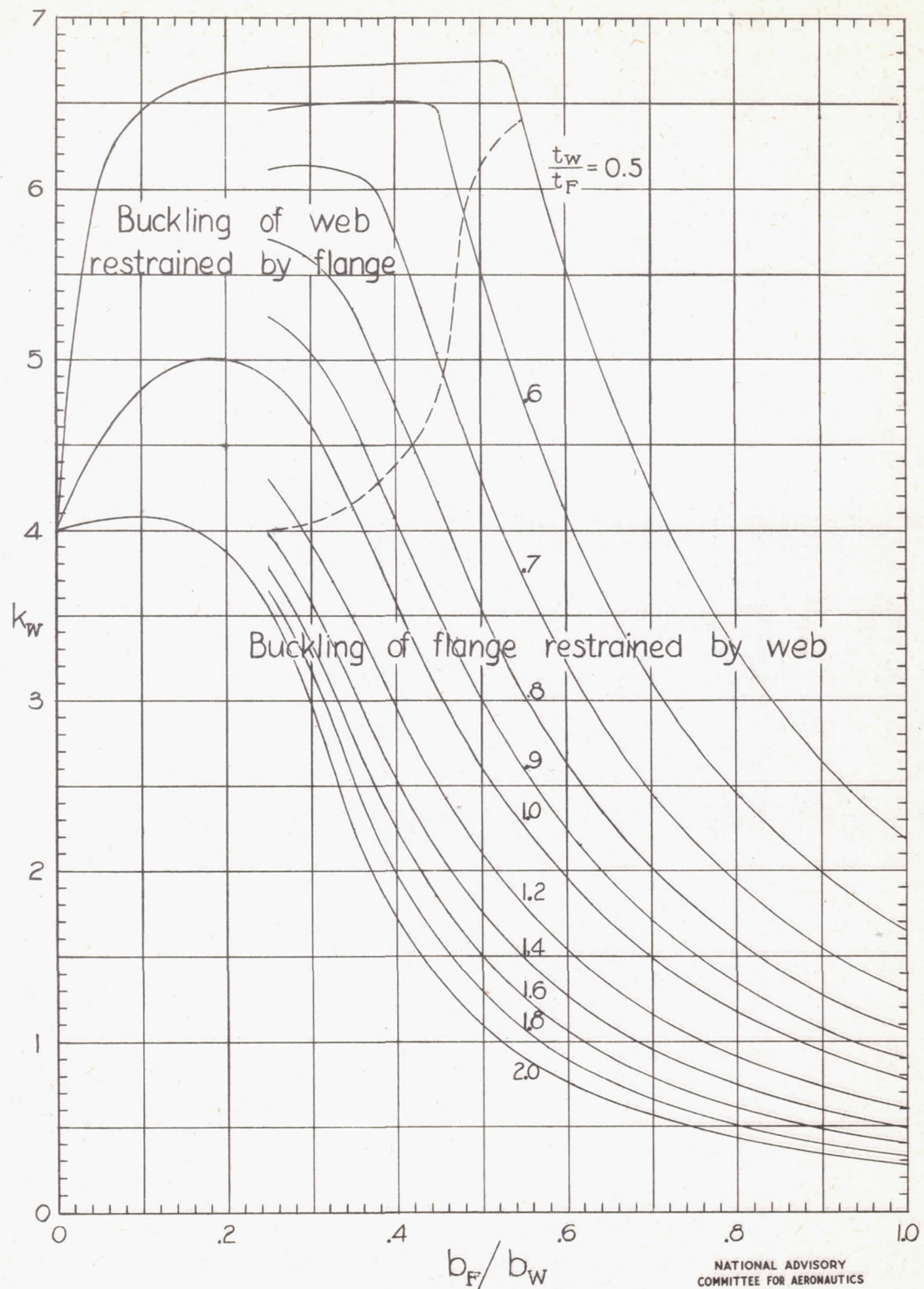
$$^a \frac{\sigma_{cr}}{\eta} = \frac{k_w n^2 E_c t_w^2}{12(1-\mu^2) b_w^2}, \text{ where } E_c = 10,700 \text{ ksi and } \mu = 0.3.$$

NATIONAL ADVISORY
COMMITTEE FOR AERONAUTICS

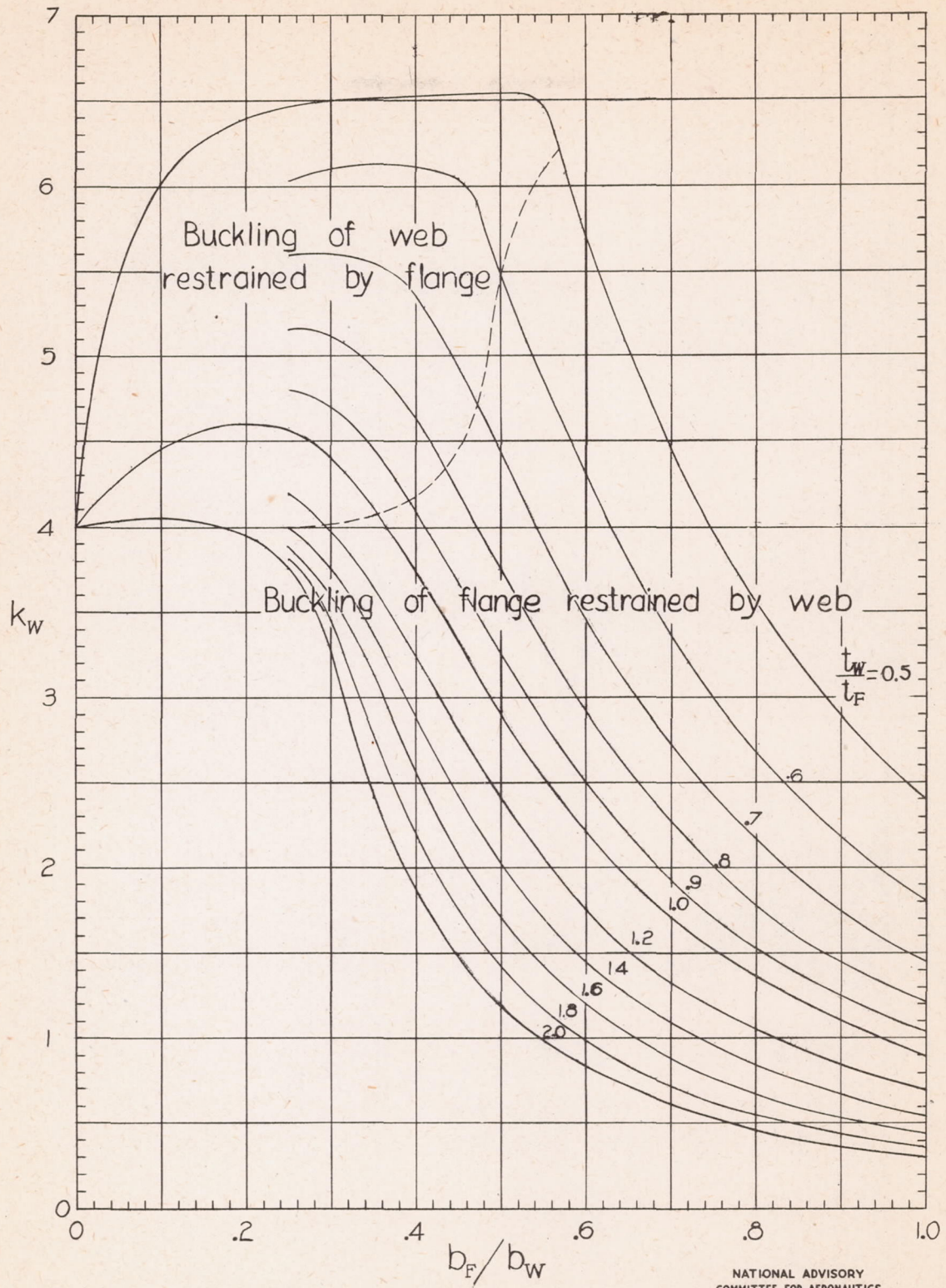


NATIONAL ADVISORY
COMMITTEE FOR AERONAUTICS

Figure 1.- Cross sections of H-, Z-, and channel-section columns.

NATIONAL ADVISORY
COMMITTEE FOR AERONAUTICSFigure 2.- Values of k_w for H-section columns. (From reference 6.)

$$\frac{\sigma_{cr}}{\eta} = \frac{k_w \pi^2 E_c t_w^2}{12(1-\mu^2) b_w^2}$$

NATIONAL ADVISORY
COMMITTEE FOR AERONAUTICSFigure 3.- Values of k_w for Z- and channel-section columns. (From reference 6.)

$$\frac{\sigma_{cr}}{\eta} = \frac{k_w \pi^2 E_c t_w^2}{12(1-\mu^2) b_w^2}$$

NACA ARR No. L6C19

Fig. 4

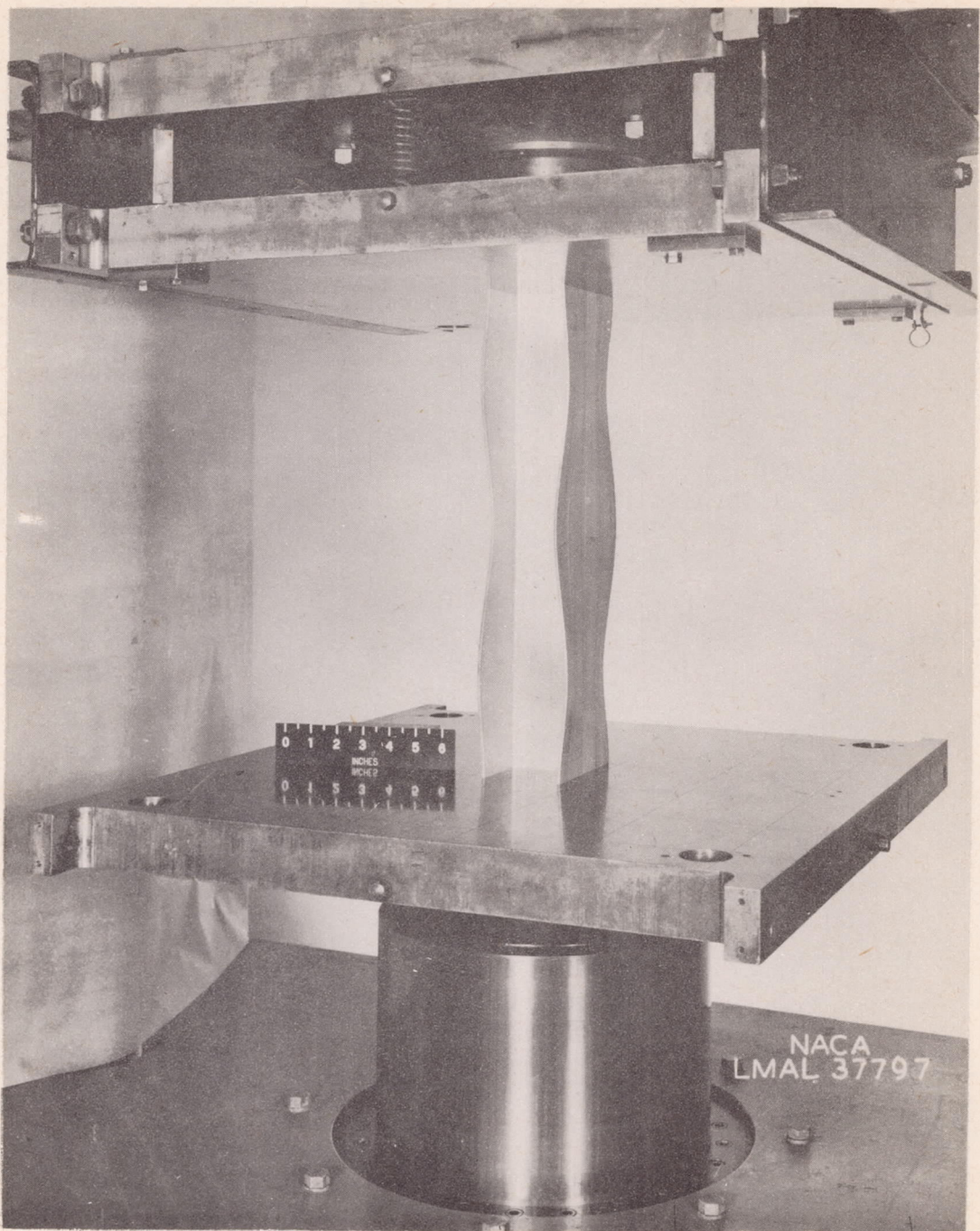


Figure 4.- Local instability of an H-section column.

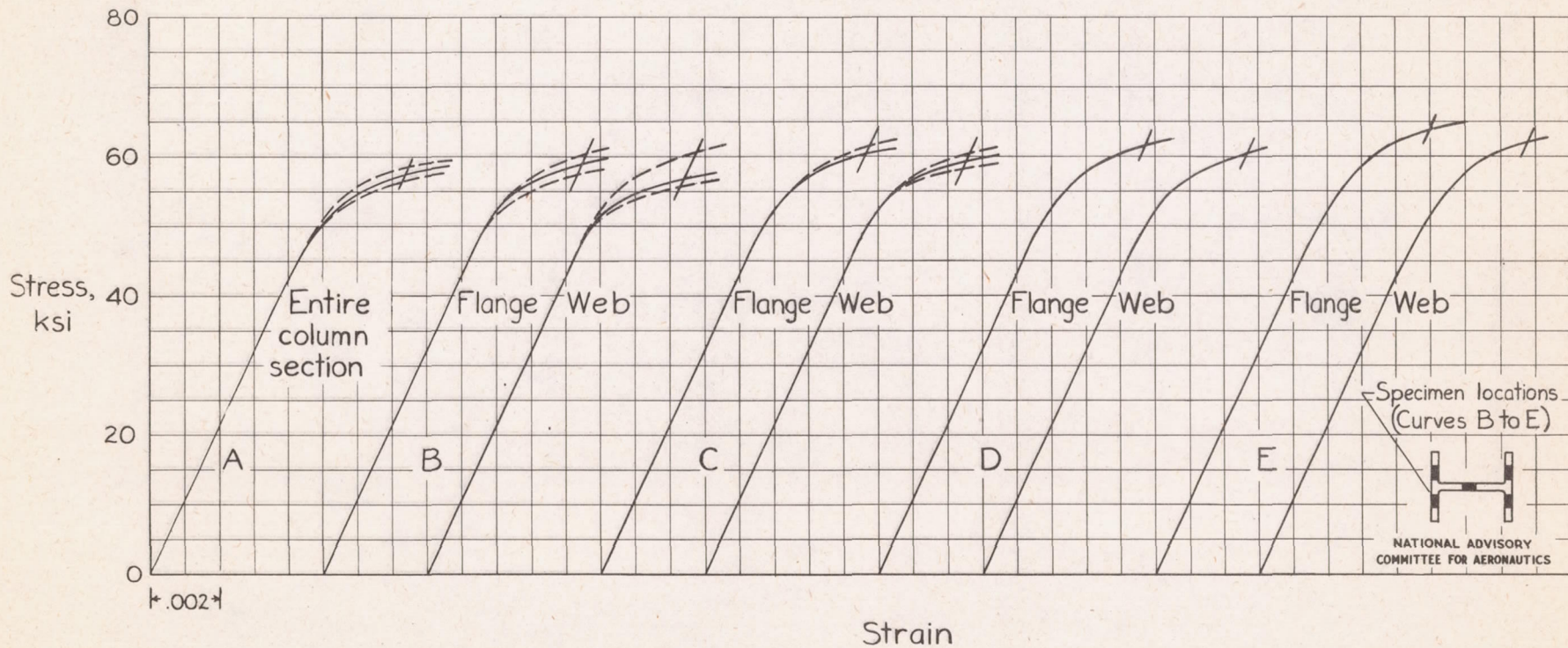
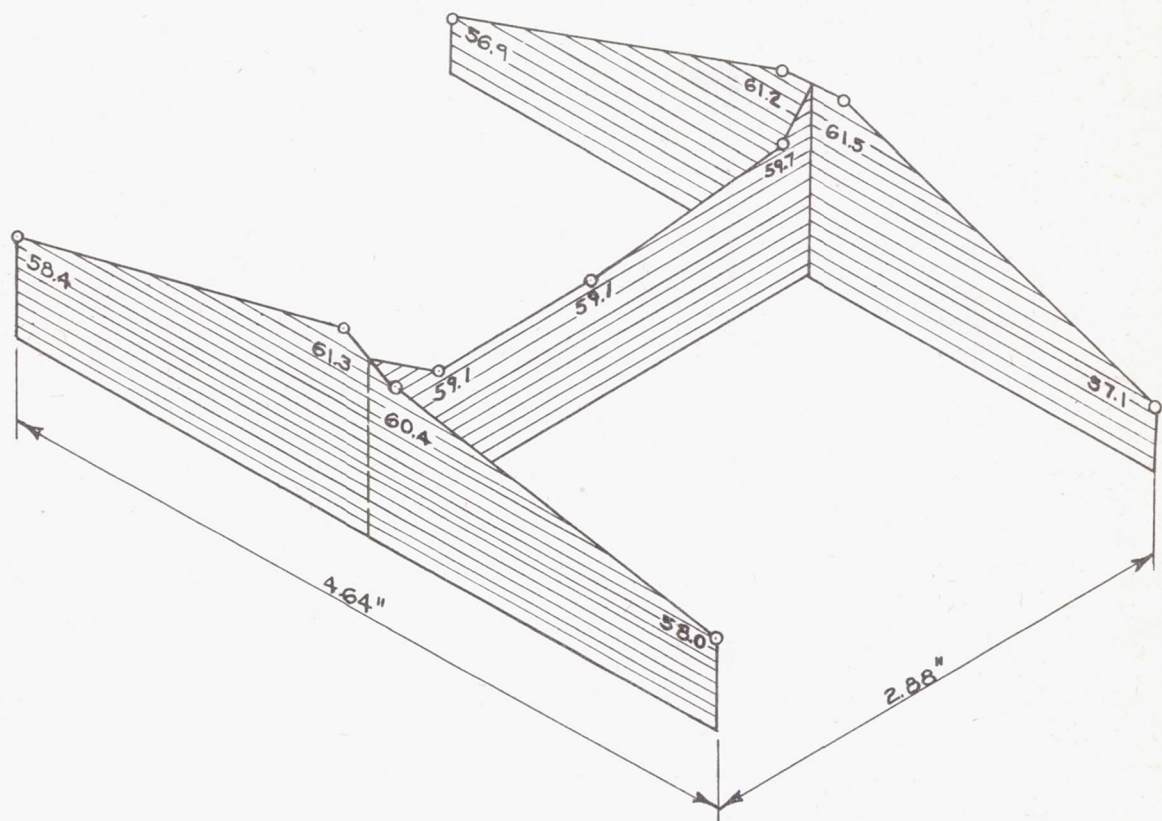


Figure 5. - Compressive stress - strain curves for extruded 14S-T aluminum alloy for with-grain direction. (Columns to which stress - strain curves B to E apply are identified in tables 1 to 3.)



NATIONAL ADVISORY
COMMITTEE FOR AERONAUTICS

Figure 6. - Variation of the compressive yield stress over a cross section of an extruded 14S-T aluminum alloy H-section with web and flanges 0.125 inch thick. (Values in ksi.)

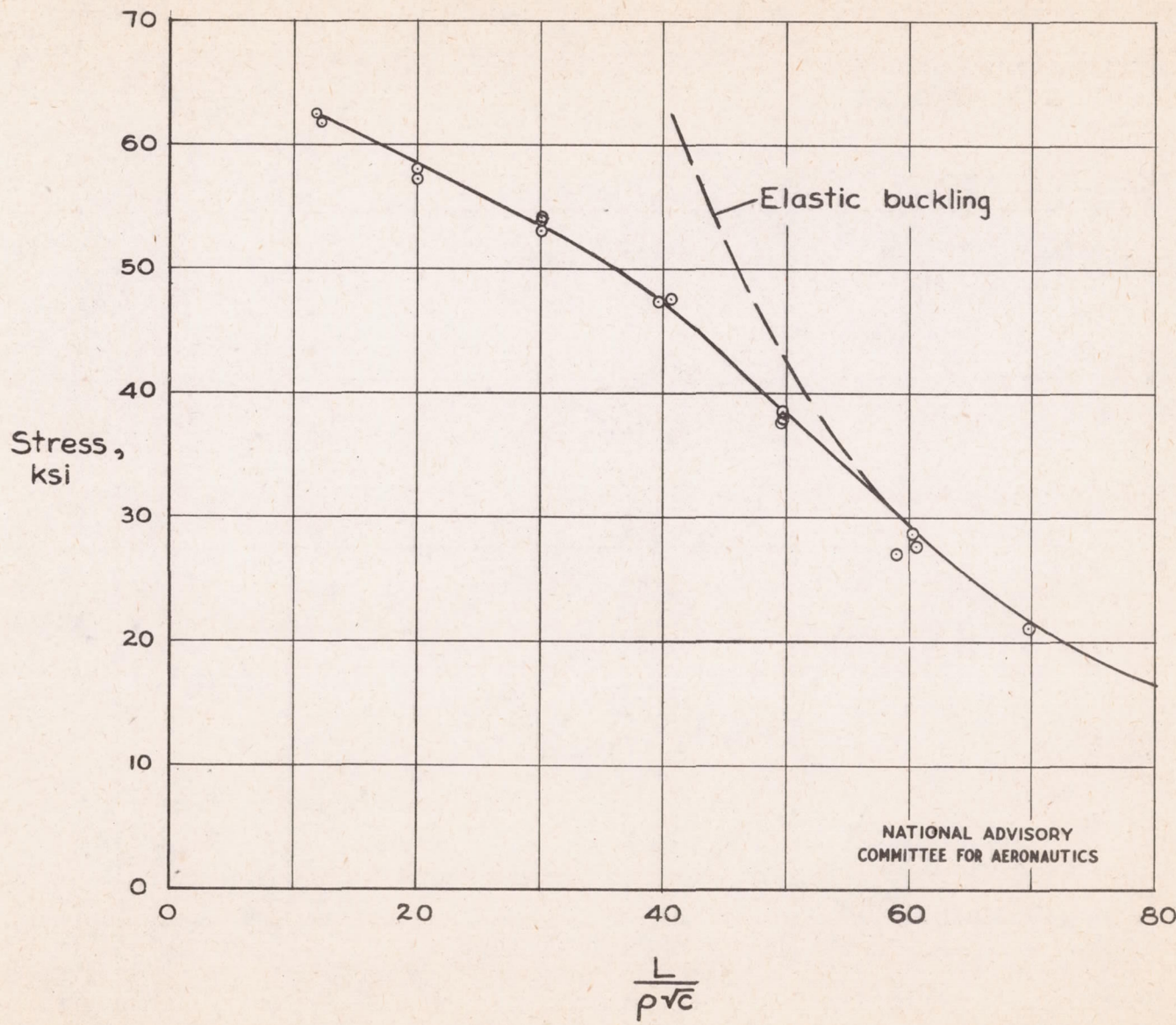
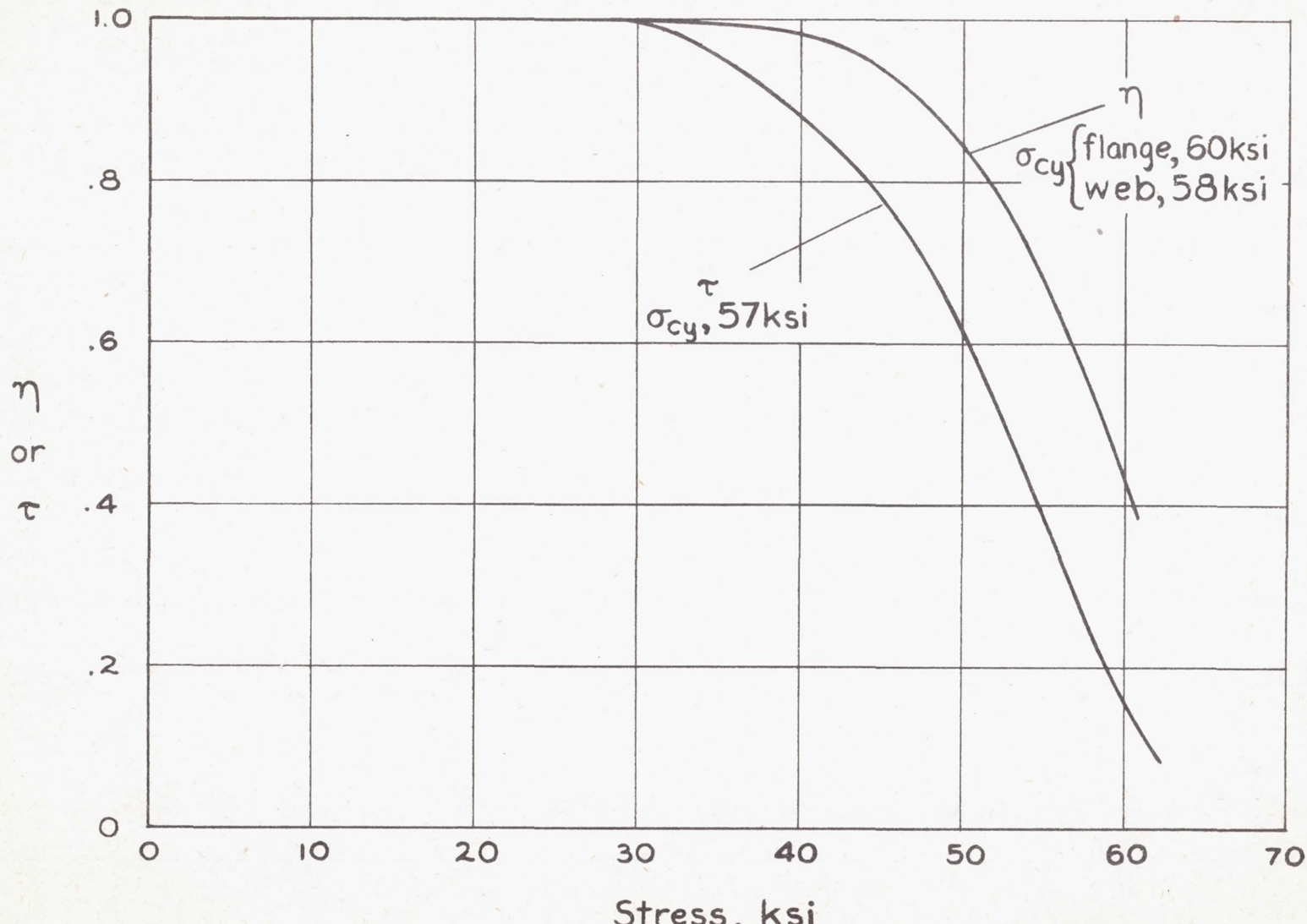
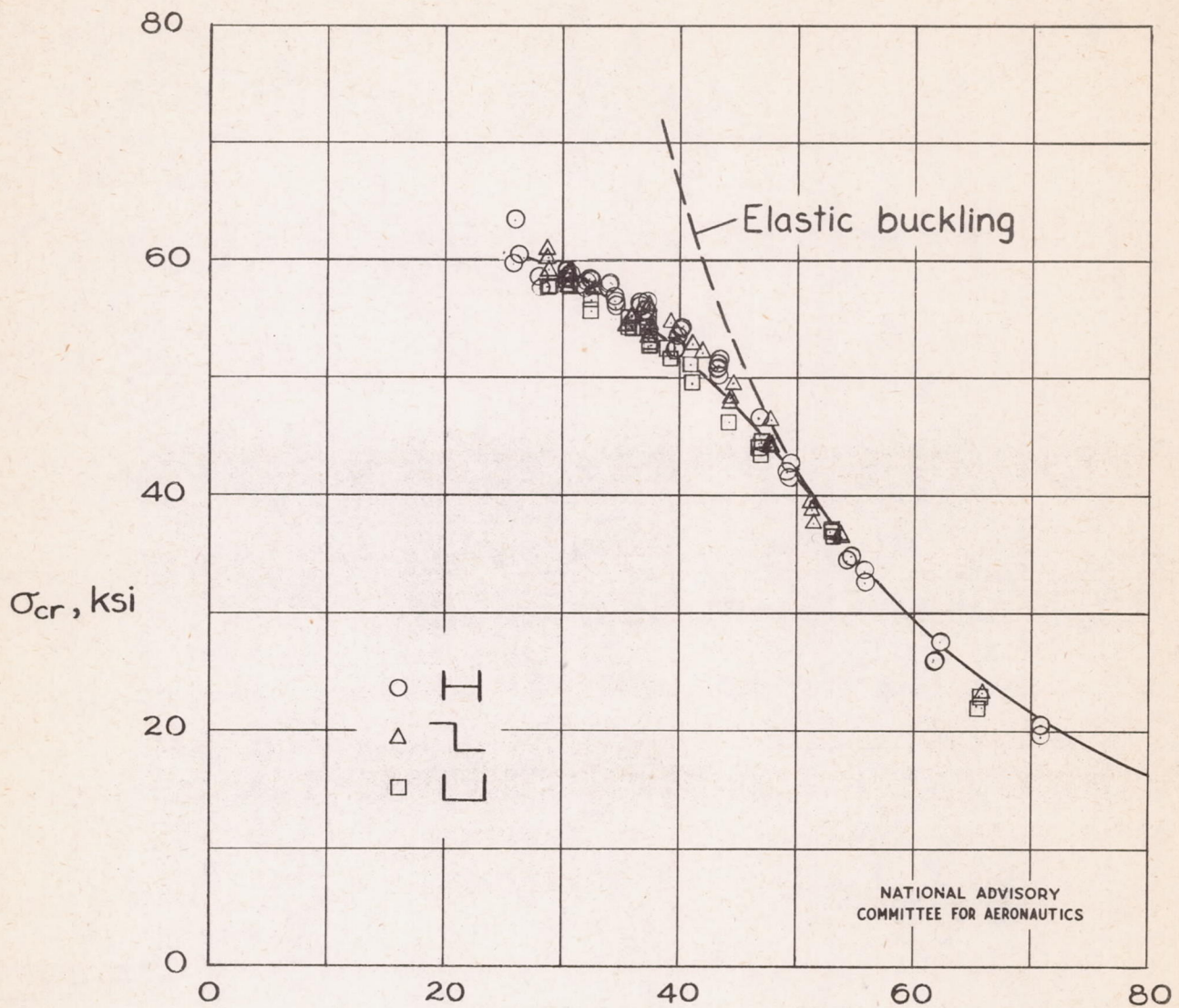


Figure 7.— Column curve for extruded 14S-T aluminum alloy obtained from tests of flat-end H-section columns. σ_{cy} , 57 ksi.



NATIONAL ADVISORY
COMMITTEE FOR AERONAUTICS

Figure 8. - Variation of τ and η with stress for extruded 14S-T aluminum alloy.



$$\frac{b_w}{t_w} \sqrt{\frac{12(1-\mu^2)}{k_w}}$$

Figure 9. - Plate-buckling curve for extruded 14S-T aluminum alloy obtained from tests of H-, Z-, and channel-section columns. σ_{cy} (flange), 60 ksi; σ_{cy} (web), 58 ksi.

Fig. 10

NACA ARR No. L6C19

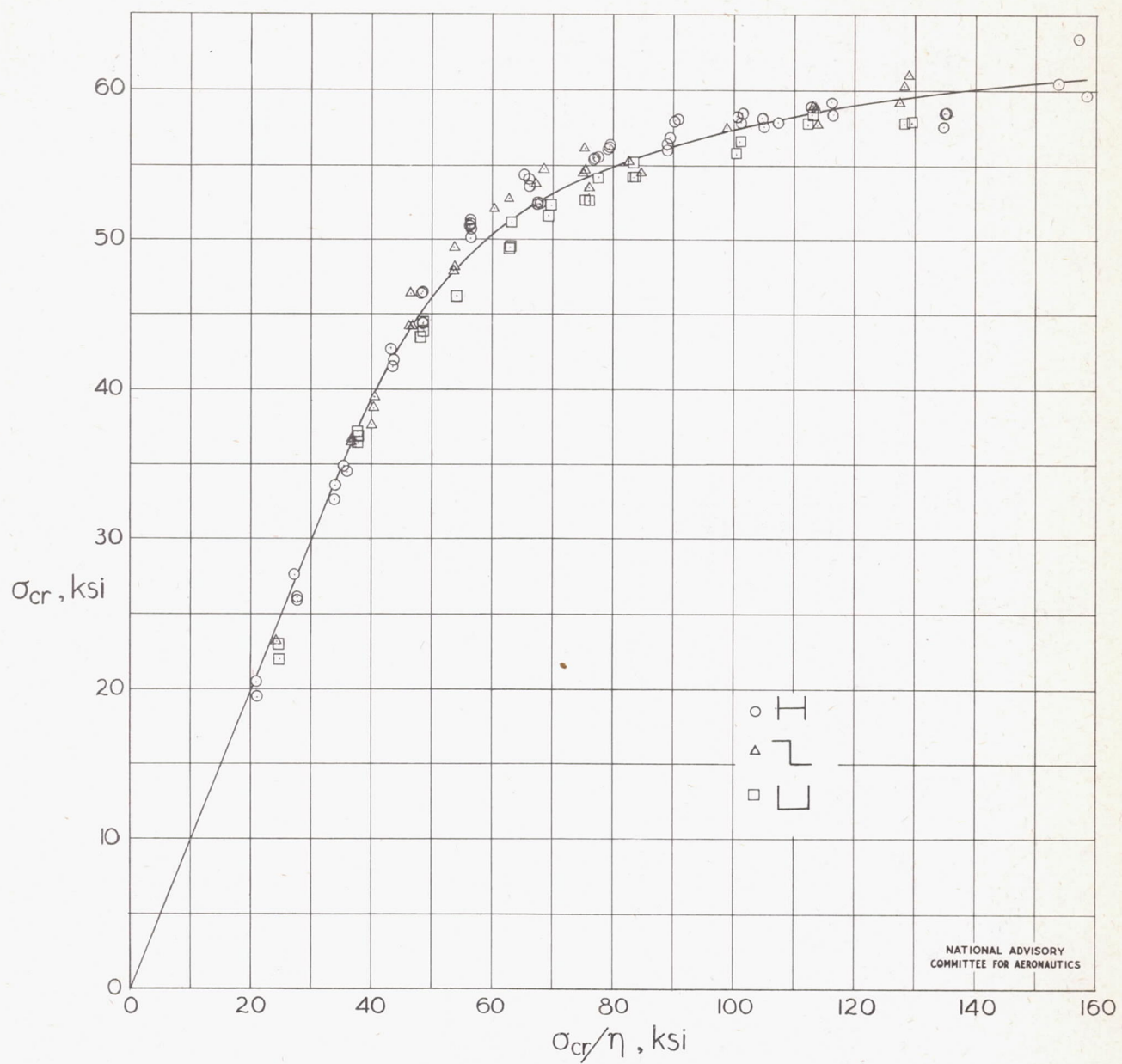


Figure 10.—Variation of σ_{cr} with σ_{cr}/η for plates of extruded 14S-T aluminum alloy obtained from tests of H-, Z-, and channel-section columns. σ_{cy} (flange), 60 ksi; σ_{cy} (web), 58 ksi.

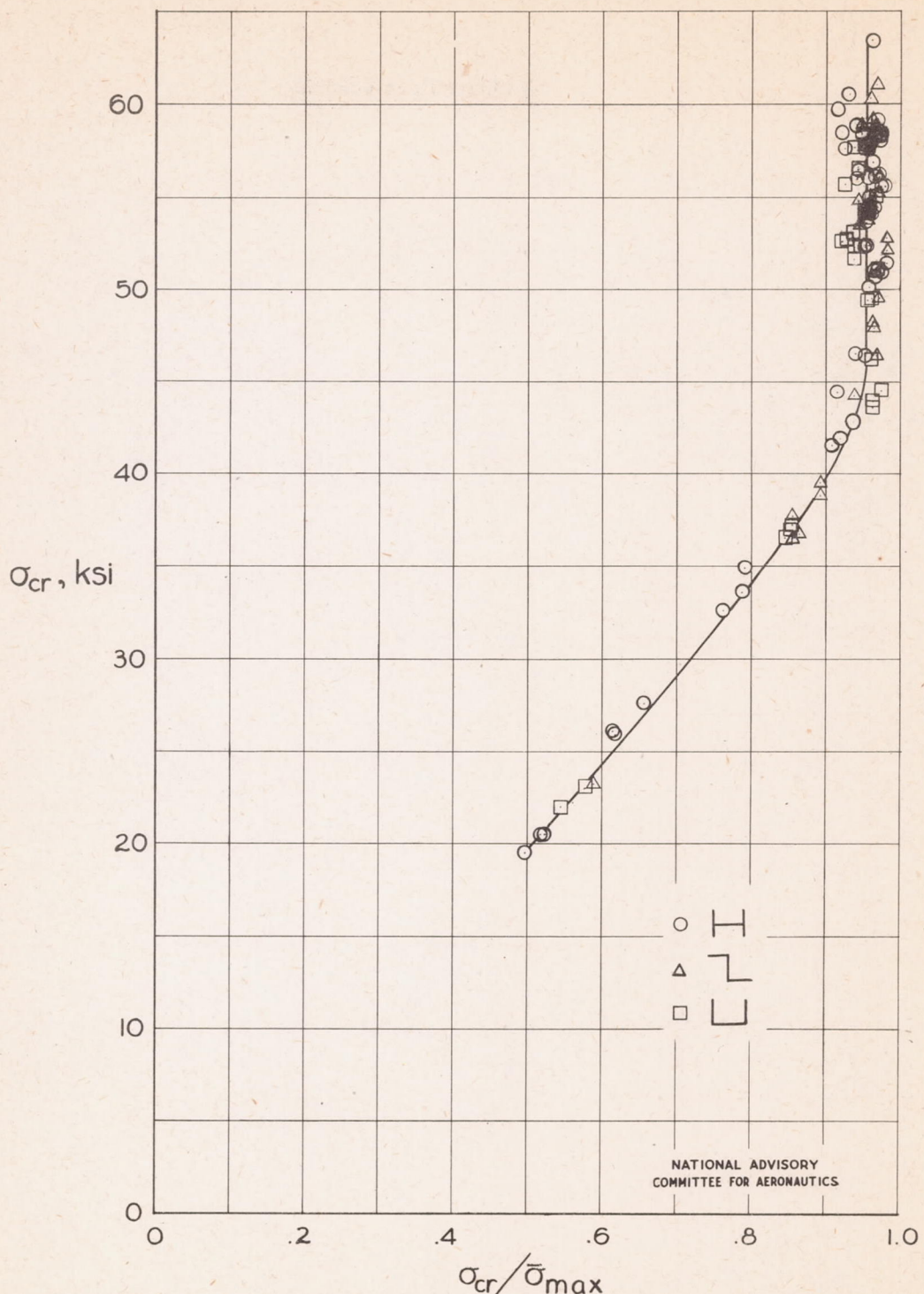


Figure 11. - Variation of σ_{cr} with $\sigma_{cr}/\bar{\sigma}_{max}$ for plates of extruded 14S-T aluminum alloy obtained from tests of H-, Z-, and channel-section columns. σ_{cy} (flange), 60 ksi; σ_{cy} (web), 58 ksi.

Fig. 12

NACA ARR No. L6C19

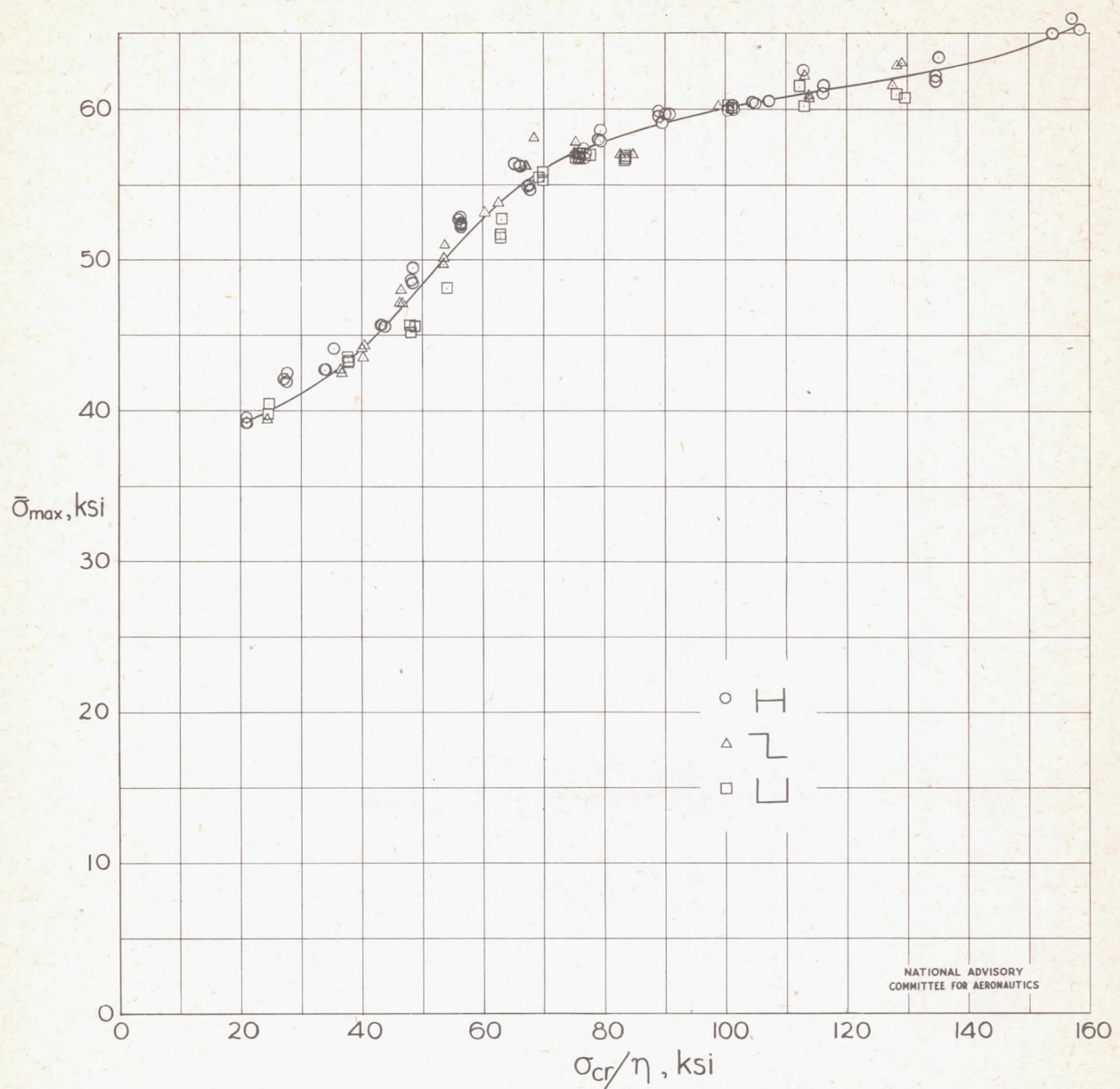


Figure 12.—Variation of $\bar{\sigma}_{\max}$ with σ_{cr}/η for plates of extruded 14S-T aluminum alloy obtained from tests of H-, Z-, and channel-section columns. σ_{cy} (flange), 60 ksi; σ_{cy} (web), 58 ksi.